WL-TR-94-2013

Modelling/Investigation of EHD Point Contacts

Farshid Sadeghi, Associate Professor
Kyung-Hoon Kim, Post Doctoral Researcher
Joe Ortiz, Graduate Assistant

Purdue Research Foundation
Purdue University
School of Mechanical Engineering
Tribology Laboratory
1288 Mechanical Engineering Building
West Lafayette IN 47907-1288

February 1994

Final Report for Period March 1992 - December 1993

APPROVED FOR PUBLIC RELEASE; DISTRIBUTION IS UNLIMITED

Aero Propulsion and Power Directorate
Wright Laboratory
Air Force Materiel Command
Wright-Patterson Air Force Base OH 45433-7103

NOTICE

When Government drawings, specifications, or other data are used for any purpose other than in connection with a definitely Government-related procurement, the United States Government incurs no responsibility or any obligation whatsoever. The fact that the government may have formulated or in any way supplied the said drawings, specifications, or other data, is not to be regarded by implication, or otherwise in any manner construed, as licensing the holder, or any other person or corporation; or as conveying any rights or permission to manufacture, use, or sell any patented invention that may in any way be related thereto.

This report is releasable to the National Technical Information Service (NTIS). At NTIS, it will be available to the general public, including foreign nations.

This technical report has been reviewed and is approved for publication.

Robert L. Wright

ROBERT L. WRIGHT, PROJ. ENG.
LUBRICATION BRANCH
FUELS AND LUBRICATION DIVISION

M Brian Bergsten

M. BRIAN BERGSTEN, ACTING CHIEF
LUBRICATION BRANCH
FUELS AND LUBRICATION DIVISION

Leo S Harootyan Jr

LEO S. HAROOTYAN, JR., Chief
Fuels & Lubrication Division
Aero Propulsion & Power Directorate

If your address has changed, if you wish to be removed from our mailing list, or if the addressee is no longer employed by your organization please notify WL/POSL , WPAFB, OH 45433-7103 to help us maintain a current mailing list.

Copies of this report should not be returned unless return is required by security considerations, contractual obligations, or notice on a specific document.

DISCLAIMER NOTICE

THIS DOCUMENT IS BEST QUALITY AVAILABLE. THE COPY FURNISHED TO DTIC CONTAINED A SIGNIFICANT NUMBER OF COLOR PAGES WHICH DO NOT REPRODUCE LEGIBLY ON BLACK AND WHITE MICROFICHE.

REPORT DOCUMENTATION PAGE

Form Approved
OMB No. 0704-0188

1. AGENCY USE ONLY (Leave blank)	2. REPORT DATE	3. REPORT TYPE AND DATES COVERED
	FEBRUARY 1994	FINAL/MAR 92 - DEC 93

4. TITLE AND SUBTITLE

MODELLING/INVESTIGATION OF EHD POINT CONTACTS

5. FUNDING NUMBERS

F33615-C-90-2086
PE 62203F
PR 3048
TA 06
WU 26

6. AUTHOR(S)

FARSHID SADEGHI, KYUNG-HOON KIM, JOE ORITZ,
PURDUE UNIVERSITY

7. PERFORMING ORGANIZATION NAME(S) AND ADDRESS(ES)

PURDUE RESEARCH FOUNDATION
DIVISION OF SPONSORED PROGRAMS
WEST LAFAYETTE IN 47907

8. PERFORMING ORGANIZATION REPORT NUMBER

9. SPONSORING/MONITORING AGENCY NAME(S) AND ADDRESS(ES)

AERO PROPULSION AND POWER DIRECTORATE
WRIGHT LABORATORY
AIR FORCE MATERIEL COMMAND
WRIGHT-PATTERSON AFB OH 45433-7103

10. SPONSORING/MONITORING AGENCY REPORT NUMBER

WL-TR-94-2013

11. SUPPLEMENTARY NOTES

12a. DISTRIBUTION/AVAILABILITY STATEMENT

Approved for public release; distribution is unlimited.

12b. DISTRIBUTION CODE

13. ABSTRACT (Maximum 200 words)

THIS STUDY WAS UNDERTAKEN TO DEVELOP A USER FRIENDLY COMPUTER MODEL TO SIMULATE HEAVILY LOADED LUBRICATED CIRCULAR AND ELLIPTIC CONTACTS, I.E., POINT CONTACTS. IN ORDER TO ACHIEVE THIS OBJECTIVE, A NUMERICAL MODEL FOR NEWTONIAN THERMAL ELASTOHYDRODYNAMIC (EHD) LUBRICATION OF ROLLING/SLIDING CONTACTS WAS DEVELOPED. THE MODEL SIMULTANEOUSLY SOLVES THE TWO-DIMENSIONAL REYNOLDS, ELASTICITY, AND THREE-DIMENSIONAL ENERGY EQUATIONS TO OBTAIN PRESSURE, FILM THICKNESS, AND TEMPERATURE DISTRIBUTION WITHIN THE LUBRICANT FILM. INTERACTIVE COMPUTER GRAPHICS ALLOW VISUALIZATION AND AID IN DESIGN AND ANALYSIS OF EHD TRIBO-CONTACTS. THIS REPORT PROVIDES A DESCRIPTION OF THE METHOD OF SOLUTION, THE COMPUTER GRAPHICS, AND A SAMPLE OF THE RESULTS.

14. SUBJECT TERMS	15. NUMBER OF PAGES
COMPUTER SIMULATION, LUBRICATION, ELASTOHYDRODYNAMIC LUBRICATION, TRIBO-CONTACTS	46
	16. PRICE CODE

17. SECURITY CLASSIFICATION OF REPORT	18. SECURITY CLASSIFICATION OF THIS PAGE	19. SECURITY CLASSIFICATION OF ABSTRACT	20. LIMITATION OF ABSTRACT
UNCLASSIFIED	UNCLASSIFIED	UNCLASSIFIED	UL

NSN 7540-01-280-5500

Standard Form 298 (Rev. 2-89)
Prescribed by ANSI Std Z39-18
298-102

FOREWORD

This report describes a U. S. Air Force sponsored project performed by Purdue Research Foundation, West Lafayette, Indiana. The project was task number 17, administered by Universal Energy Systems, Dayton, Ohio under government contract number F33615-90-C-2086, "Short-term Propulsion and Power Development Analysis/Assessment and Information Dissemination." Mr. Robert Wright, WL/POSL, was the government project task monitor, while Mr. Curtis Reeves, WL/POMX, was the government contract monitor.

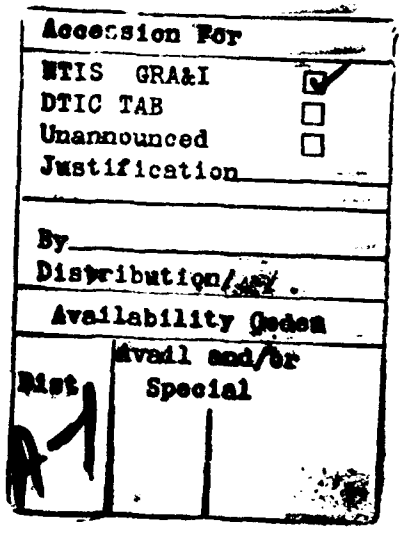

Table of Contents

List of Figures

List of Symbols

a	Half width of the Hertzian contact in Y-direction, m
b	Half width of the Hertzian contact in X-direction, m
C_1	Dimensionless constant, $\frac{k_f}{\sqrt{\pi \rho_{os} C_{ps} u_1 k_s b}}$
C_2	Dimensionless constant, $\frac{k_f}{\sqrt{\pi \rho_{os} C_{ps} u_2 k_s b}}$
C_{pf}	Specific heat of the lubricant, J/(kg – ° K)
C_{ps}	Specific heat of the solids, J/(kg – ° K)
E	Young's modulus, Pa
E'	Equivalent Young's modulus $\frac{1}{E'} = \frac{1}{2}\left[\frac{1-\nu_1^2}{E_1} + \frac{1-\nu_2^2}{E_2}\right]$, Pa
f	Load, N
G	Material parameter, $\alpha E'$
h	Film thickness, m
H	Dimensionless film thickness, hR/b^2
H_1	Dimensionless film thickness, h/b
H_o	Dimensionless constant used in calculation of H
K	Dimensionless constant, $\frac{k_f}{\rho_{of} U_m b C_{pf}}$
k_f	Thermal conductivity of the lubricant, W/[m – °K]
k_s	Thermal conductivity of the solids, W/[m – °K]
k_e	Ellipticity parameter, a/b
p	Pressure, Pa
P	Dimensionless pressure, p/P_H
P_H	Maximum Hertzian pressure, Pa
r	Radius ratio, R_y/R_x
R_x	Equivalent radius of the contact in x-direction $1/R_x = 1/R_{x1} + 1/R_{x2}$, m
R_y	Equivalent radius of the contact in y-direction $1/R_y = 1/R_{y1} + 1/R_{y2}$, m
s	Slide to roll ratio (slip)

S_o	Exponent in the viscosity equation, $= \frac{\delta(T_o - 138)}{\ln(\mu_o) + 9.67}$
t	Temperature, °K
T	Dimensionless temperature, t / T_o
T_o	Inlet temperature, ° K
T_1	Dimensionless temperature at surface 1
T_2	Dimensionless temperature at surface 2
u	Velocity in x-direction, m/sec
u_1	Velocity at surface 1, m/sec
u_2	Velocity at surface 2, m/sec
u_m	Average velocity, $\frac{u_1 + u_2}{2}$, m/sec
U	Dimensionless velocity in the X-direction, u/u_m
U*	Dimensionless speed parameter, $\frac{\eta_o u_m}{E'R_x}$
v	Velocity in the y-direction, m/sec
V	Dimensionless velocity in the Y-direction, v/u_m
w	Velocity in z-direction, m/sec
W	Dimensionless velocity in the Z_1-direction, w/u_m
W*	Dimensionless load parameter, $f/E'R_x^2$
x	Coordinate along the rolling direction, m
X	Dimensionless coordinate along the rolling direction, x/b
X′	Dummy variable
X_s	Inlet position
y	Coordinate perpendicular to the rolling direction on the plane of contact, m
Y	Dimensionless coordinate perpendicular to the rolling direction, y/b
Y_1	Dimensionless coordinate perpendicular to the rolling direction, y/a
Y′	Dummy variable
z	Coordinate in the film thickness direction, m
Z	Dimensionless coordinate in the film thickness direction, zR/b^2
Z_1	Dimensionless coordinate in the film thickness direction, z/b
$\tilde{Z}$	Dummy variable

α	Pressure viscosity coefficient, m^2/N
β	Thermal expansivity of lubricant, $°K^{-1}$
$\tilde{\beta}$	Dimensionless constant, $\frac{P_H \beta}{\rho_{of} C_{pf}}$
γ	Temperature-viscosity coefficient, $°K^{-1}$
δ	Constant in the viscosity equation
λ_1	Dimensionless velocity parameter, $\frac{\eta_o u_1 R^2}{b^3 P_H}$
λ_2	Dimensionless velocity parameter, $\frac{\eta_o u_2 R^2}{b^3 P_H}$
Λ	Dimensionless constant, b/R
ν	Poisson's ratio
η_o	Ambient viscosity of the lubricant, N–sec/m^2
$\bar{\eta}$	Viscosity of lubricant, N-sec /m^2
η	Dimensionless viscosity, $\bar{\eta}/\eta_o$
ρ_{of}	Ambient density of the lubricant, kg/m^3
ρ_{os}	Density of the solids, kg/m^3
$\bar{\rho}$	Density of lubricant, kg/m^3
ρ	Dimensionless density, $\bar{\rho}/\rho_o$
μ	Dimensionless constant, $\frac{\eta_o u_m}{\rho_{of} T_o b C_{pf}}$
ξ	Dummy variable
ψ	Roelands pressure viscosity exponent

Subscripts

1	Surface 1 unless specified otherwise
2	Surface 2 unless specified otherwise

1. Objective

The objective of this study was to develop a user friendly model to investigate heavily loaded lubricated circular and noncircular (elliptic) contacts. In order to achieve the objectives, a numerical model for the Newtonian thermal elastohydrodynamic lubrication (EHD) of rolling/sliding point contacts was developed. The model simultaneously solves the two-dimensional Reynolds, Elasticity and the three-dimensional energy equations to obtain the pressure, film thickness and temperature distribution within the lubricant film. The numerical model was extended with an interactive computer graphics to aid in the design and analysis of elastohydrodynamic lubrication of rolling/sliding tribo-contacts. This report provides a description of the method of solution, the computer aided design graphics package and a sample of the results.

2. Introduction

The lubrication of heavily loaded high speed machine components such as bearings, gears, etc., has been extensively investigated in recent years. However, most of the analyses have routinely assumed the lubrication process to be isothermal. Most of the research and published works have dealt with isothermal and thermal EHD lubrication of line contacts or isothermal EHD of point contacts. The study of heavily loaded lubricated line contacts with the thermal effects included started with Sternlicht et al. in 1961. Cheng (1965) investigated the thermal effects in EHD lubrication of line contact, however, the loads considered in his analysis were extremely low which resulted in insignificant temperature rise. Murch and Wilson (1975) illustrated that temperature will significantly affect the film thickness particularly at high speeds. Sadeghi and Dow (1987) used experimental pressure and surface temperature measurements to investigate the temperature rise within the lubricant film operating under EHD lubrication. They illustrated that the temperature rise is significant and cannot be neglected. Recently, Sadeghi and Sui (1990) developed a complete numerical solution to the EHD lubrication of line contacts.

The EHD lubrication of point contacts has been investigated less rigorously. This is mainly due to the extreme complexity involved in the solution of the two-dimensional Reynolds and elasticity equations. Many investigators have studied the isothermal EHD lubrication of point contacts, for example, Ranger, Ettles and Cameron (1975), Hamrock and Dowson (1977), and Evans and Snidle (1982). However, most of these analyses are extremely computer time intensive. Recently, Lubrecht et al. (1987) used multigrid technique to solve EHD lubrication of point contacts. This method provided a fast converging scheme, however, they neglected the thermal effects within the lubricant film. Brüggemann and Kollmann (1982) are among the first to include the thermal effects in EHD lubrication of point contacts. They only considered the

conduction across the film and viscous dissipation. They chose to neglect compression heating/cooling and convection terms. However, it has been shown (Sadeghi and Sui, 1990) that compression heating/cooling plays a major role in EHD lubrication and since the Peclet number is usually high the convection term cannot be neglected. They also assumed a pressure distribution rather than solving the Reynolds equation. Zhu and Wen (1984) presented a solution for thermal EHD lubrication of point contacts. However, the loads considered in their analysis were extremely low. Blahey and Schneider (1986) also developed a solution for the thermal EHD lubrication of elliptic contacts using control volume approach. However, they also neglected the convection term in the energy equation. Recently, Faghri (1984) presented a methodology for finite difference solutions of two-dimensional convection-diffusion problems in irregular domains, using a non-orthogonal coordinate transformation.

In this report, the graphics package for the EHD analysis and the technique used to solve the three-dimensional energy equation for thermal EHD lubrication of point contact under rolling/sliding condition is described.

3. Mathematical Formulation

Figure 1 illustrates a schematic of the problem under consideration. The lower body (flat plate) and the upper body (an ellipsoid) are moving at the surface velocities of u_1 and u_2, respectively. Lubricant is pulled into the contact due to the viscous effects of the lubricant and the movement of the bodies. The load causes the pressure within the lubricant film to elastically deform the bounding surfaces.

Reynolds Equation

The dimensionless Newtonian thermal Reynolds equation with the appropriate assumptions derived from the Navier-Stokes equation can be written as [Dowson,1962]:

$$\frac{\partial}{\partial X}\left[\tilde{\rho}H^3\frac{\partial P}{\partial X}\left(G_1-G_2\right)\right]+\frac{\partial}{\partial Y}\left[\tilde{\rho}H^3\frac{\partial P}{\partial Y}\left(G_1-G_2\right)\right]+\left(\lambda_2-\lambda_1\right)\frac{\partial}{\partial X}\left(\tilde{\rho}\,H\,G_3\right)+\lambda_1\frac{\partial}{\partial X}\left(\tilde{\rho}HG_4\right)=0 \tag{1}$$

where

$$G_1=\int_0^1 F_1(T)\int_0^Z\frac{\tilde{Z}}{\eta}\,d\tilde{Z}\,dZ \tag{2}$$

$$G_2=\frac{\int_0^1\frac{Z}{\eta}\,dZ}{\int_0^1\frac{dZ}{\eta}}\int_0^1 F_1(T)\int_0^Z\frac{d\tilde{Z}}{\eta}\,dZ \tag{3}$$

$$G_3=\frac{\int_0^1 F_1(T)\int_0^Z\frac{d\tilde{Z}}{\eta}\,dZ}{\int_0^1\frac{dZ}{\eta}}, \tag{4}$$

$$G_4=\int_0^1 F_1(T)\,dZ, \tag{5}$$

$$F_1(T)=1-\beta\,T_o\,(T-1), \tag{6}$$

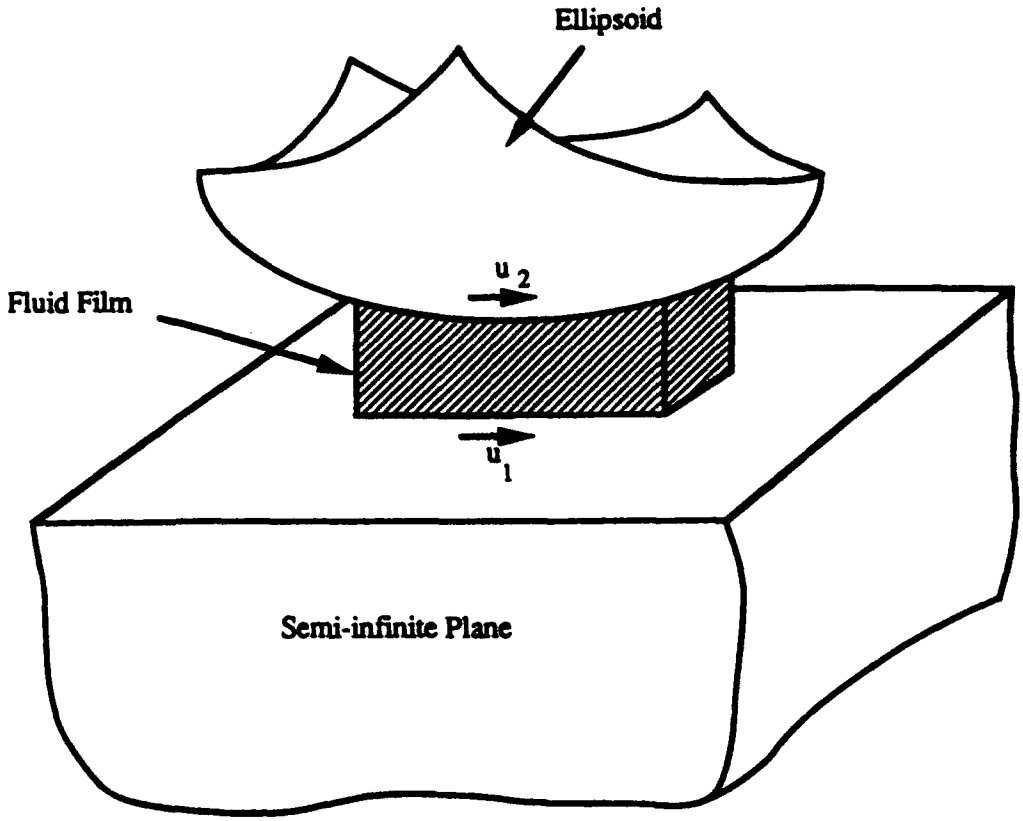

Figure 1. Lubricated contact of an ellipsoid and a semi-infinite plane.

$$\tilde{\rho} = \rho \quad \text{at } T = 1, \tag{7}$$

The boundary conditions for equation (1) are:

$$P = 0 \quad \text{on the periphery} \tag{8}$$

$$P = \frac{\partial P}{\partial X} = \frac{\partial P}{\partial Y} = 0 \quad \text{on the cavitation boundary} \tag{9}$$

The constant load condition is:

$$\int_{-\infty}^{\infty}\int_{-\infty}^{\infty} P\, dX\, dY = \frac{2\pi k_e}{3} \tag{10}$$

Energy Equation

The Reynolds equation is two-dimensional, however, the energy equation is three-dimensional because of the temperature variation in the Z_1-direction (Figure 2). The energy equation in dimensionless form is[Sherman, 1990]:

$$\rho\left[U\frac{\partial T}{\partial X} + V\frac{\partial T}{\partial Y} + W\frac{\partial T}{\partial Z_1}\right] - K\left[\frac{\partial^2 T}{\partial X^2} + \frac{\partial^2 T}{\partial Y^2} + \frac{\partial^2 T}{\partial Z_1^2}\right] = \mu\eta\left[\left[\frac{\partial U}{\partial Z_1}\right]^2 + \left[\frac{\partial V}{\partial Z_1}\right]^2\right] + \tilde{\beta}\, T\left[U\frac{\partial P}{\partial X} + V\frac{\partial P}{\partial Y}\right] \tag{11}$$

The dimensionless boundary conditions for the energy equation (11) are (Carslaw and Jaeger ,1959 and Zhu and Cheng, 1989):

$$T_1(X,Y) = C_1 \int_{X_s}^{X} \left[\frac{\partial T}{\partial Z_1}\right]_{Z_1=0} \frac{d\xi}{(X-\xi)^{1/2}} \tag{12}$$

$$T_2(X,Y) = C_2 \int_{X_s}^{X} \left[\frac{\partial T}{\partial Z_1}\right]_{Z_1=\Delta H} \frac{d\xi}{(X-\xi)^{1/2}} \tag{13}$$

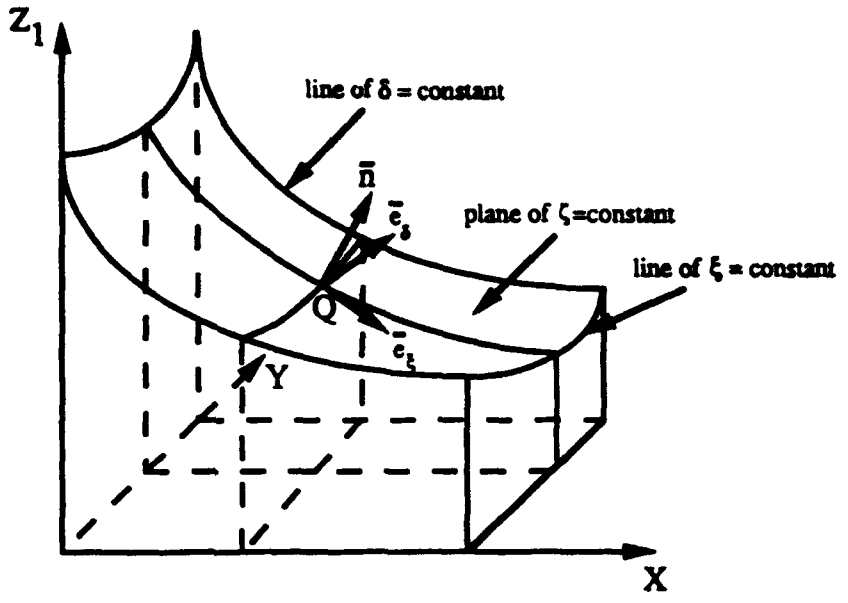

(a) Physical domain.

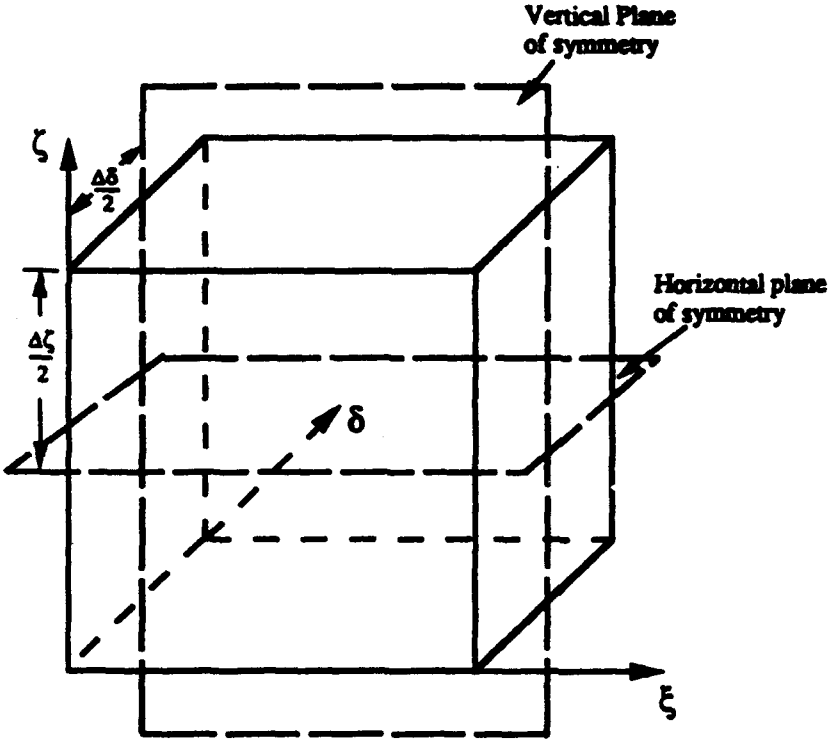

(b) Transformed domain.

Figure 2. Coordinate trasnformation.

Film Thickness Equation

The elastic deformation of the surfaces in dimensionless form is given by:

$$H(X,Y) = H_o + \frac{X^2 + Y^2/r}{2} + \frac{2\theta_1}{\pi^2}\int\int \frac{P dX' dY'}{[(X-X')^2 + (Y-Y')^2]^{1/2}} \tag{14}$$

where, $\theta_1 = \dfrac{\pi P_H R_x}{E' b}$

Viscosity-Pressure-Temperature Relationship

The viscosity/pressure relationship used in this analysis was proposed by Roelands (1963) and further developed by Houpert(1985). The Roelands equation in dimensionless form is:

$$\eta = \exp\left\{\left[\left[\ln(\eta_o) + 9.67\right]\right]\left[\left[\frac{T_o\,T - 138}{T_o - 138}\right]^{-S_o}\left[1 + 5.1\times 10^{-9}\,P_H\,P\right]^{w} - 1\right]\right\} \tag{15}$$

Density-Pressure-Temperature Relationship

The density/pressure relationship used by Dowson and Higginson (1966) in the dimensionless form is employed in this analysis.

$$\rho = \left[1 + \frac{0.6\times 10^{-9}\,P_H P}{1 + 1.7\times 10^{-9}\,P_H P}\right]\left[1 - \beta\,T_o(T-1)\right] \tag{16}$$

Coordinate Transformation

The energy equation (11) requires a coordinate transformation due to the curved boundary before control volume formulation can be applied. The transformation equations used in this study are:

$$\xi = X, \quad \delta = Y, \quad \text{and} \quad \zeta = \frac{Z_1}{\Lambda H(X,Y)} \tag{17}$$

The unit vectors along the new coordinates are $\vec{e}_\xi$, $\vec{e}_\delta$, and $\vec{e}_\zeta$ where $\vec{e}_\zeta = \vec{e}_Z$. Figure 2a illustrates the unit vector $\vec{n}$ normal to the curved plane of ζ = constant at a point Q:

$$\vec{n} = \frac{\nabla\zeta}{|\nabla\zeta|} = \frac{-\bar{\beta}\,\vec{e}_X - \bar{\gamma}\vec{e}_Y + \vec{e}_Z}{\bar{\alpha}} \tag{18}$$

where $\bar{\alpha} = \sqrt{1+\bar{\beta}^2+\bar{\gamma}^2}$, $\bar{\beta} = \Lambda\zeta\frac{\partial H}{\partial\xi}$ and $\bar{\gamma} = \Lambda\zeta\frac{\partial H}{\partial\delta}$

The unit vector $\vec{n}$ is perpendicular to the line of constant ξ and line of constant δ passing through the point Q, therefore the unit vectors $\vec{e}_\xi$ and $\vec{e}_\delta$ are,

$$\vec{e}_\xi = \frac{\vec{e}_X + \bar{\beta}\,\vec{e}_Z}{\sqrt{1+\bar{\beta}^2}} \tag{19}$$

and

$$\vec{e}_\delta = \frac{\vec{e}_Y + \bar{\gamma}\,\vec{e}_Z}{\sqrt{1+\bar{\gamma}^2}} \tag{20}$$

The velocity vector in the new coordinate system is

$$\vec{U} = U_\xi\,\vec{e}_\xi + V_\delta\,\vec{e}_\delta + W_\zeta\vec{e}_\zeta \tag{21}$$

and the velocity components are

$$U_\xi = \sqrt{1+\bar{\beta}^2}\;U$$

$$V_\delta = \sqrt{1+\bar{\gamma}^2}\;V \tag{22}$$

$$W_\zeta = W - \bar{\beta}U - \bar{\gamma}V$$

The partial derivates in terms of transformed coordinates are

$$\frac{\partial}{\partial X} = \frac{\partial}{\partial \xi} - \frac{\bar{\beta}}{\Lambda H}\frac{\partial}{\partial \zeta}$$

$$\frac{\partial}{\partial Y} = \frac{\partial}{\partial \delta} - \frac{\bar{\gamma}}{\Lambda H}\frac{\partial}{\partial \zeta} \qquad (23)$$

$$\frac{\partial}{\partial Z_1} = \frac{1}{\Lambda H}\frac{\partial}{\partial \zeta}$$

and the gradient operator ∇ is:

$$\nabla = \left[\frac{\partial}{\partial \xi} - \frac{\bar{\beta}}{\Lambda H}\frac{\partial}{\partial \zeta}\right]\vec{e}_X + \left[\frac{\partial}{\partial \delta} - \frac{\bar{\gamma}}{\Lambda H}\frac{\partial}{\partial \zeta}\right]\vec{e}_Y + \left[\frac{1}{\Lambda H}\frac{\partial}{\partial \zeta}\right]\vec{e}_Z \qquad (24)$$

Control Volume Formulation and Discretization

The Reynolds equation (1) can be expressed in integral form as:

$$\int_A \nabla \cdot \left[\tilde{\rho} H^3 \left(G_1 - G_2\right) \nabla P\right] dA + \int_A \left(\lambda_2 - \lambda_1\right)\frac{\partial}{\partial X}\left[\tilde{\rho}\, H\, G_3\right] dA + \int_A \lambda_1 \frac{\partial}{\partial X}\left[\tilde{\rho}\, H\, G_4\right] dA = 0 \qquad (25)$$

Using the divergence theorem, equation (25) can be rewritten as

$$\int_A \vec{n} \cdot \left[\tilde{\rho} H^3 \left(G_1 - G_2\right) \nabla P\right] dS + \int_A \left(\lambda_2 - \lambda_1\right)\frac{\partial}{\partial X}\left[\tilde{\rho}\, H\, G_3\right] dA + \int_A \lambda_1 \frac{\partial}{\partial x}\left[\tilde{\rho}\, H\, G_4\right] dA = 0 \qquad (26)$$

Equation (26) integrated over a control volume element dA on the X-Y plane (Figure 3a) yields:

$$\tilde{\rho} H^3 \left(G_1 - G_2\right)\frac{\partial P}{\partial X}\Big|_2 \Delta Y - \tilde{\rho} H^3 \left(G_1 - G_2\right)\frac{\partial P}{\partial X}\Big|_1 \Delta Y + \tilde{\rho} H^3 \left(G_1 - G_2\right)\frac{\partial P}{\partial Y}\Big|_4 \Delta X -$$

$$\tilde{\rho} H^3 \left(G_1 - G_2\right)\frac{\partial P}{\partial Y}\Big|_3 \Delta X + \left(\lambda_2 - \lambda_1\right)\frac{\partial}{\partial X}\left[\tilde{\rho} H G_3\right]\Delta X \Delta Y + \lambda_1 \frac{\partial}{\partial X}\left[\tilde{\rho} H G_4\right]\Delta X \Delta Y = 0 \qquad (27)$$

where the numeral subscript of the vertical lines denotes the intermediate point between the

nodal point of the calculation and the neighboring points. The central difference scheme was used to discretize equation (27), however, the last two terms in the equation were discretized using the backward difference scheme. This provided a stable solution for the heavily loaded case. The energy equation (11) expressed in integral form is:

$$\int \left[\frac{\partial \left[\rho U T\right]}{\partial X} + \frac{\partial \left[\rho V T\right]}{\partial Y} + \frac{\partial \left[\rho W T\right]}{\partial Z_1} \right] d\tilde{V} - K \int \left[\frac{\partial^2 T}{\partial X^2} + \frac{\partial^2 T}{\partial Y^2} + \frac{\partial^2 T}{\partial Z_1^2} \right] d\tilde{V}$$

$$- \mu \int \eta \left[\left(\frac{\partial U}{\partial Z_1} \right)^2 + \left(\frac{\partial V}{\partial Z_1} \right)^2 \right] d\tilde{V} - \tilde{\beta} \int T \left[U \frac{\partial P}{\partial X} + V \frac{\partial P}{\partial Y} \right] d\tilde{V} = 0 \qquad (28)$$

or in vector form,

$$\int \nabla \cdot \left[\rho T \vec{U} \right] d\tilde{V} - K \int \nabla^2 T \, d\tilde{V} - S' = 0 \qquad (29)$$

where S' denotes the last two terms in equation (28). Applying the divergence theorem to equation (29) yields:

$$\int_A (\vec{U} \cdot \vec{n}) \rho T \, dA - K \int_A \vec{n} \cdot \nabla T \, dA - S' = 0 \qquad (30)$$

In order to evaluate the surface integrals, expressions for the surface area dA, the gradient operator ∇, and the unit vector $\vec{n}$ are needed.

For surface 1 (Figure 3b),

$$\vec{n} = -\vec{e}_x, \quad \vec{U} \cdot \vec{n} = -U \qquad (31)$$

$$\vec{n} \cdot \nabla T = -\frac{\partial T}{\partial \xi} + \frac{\tilde{\beta}}{\Lambda H} \frac{\partial T}{\partial \zeta}$$

and $dA = \Lambda H \, d\delta \, d\zeta$

For surface 3,

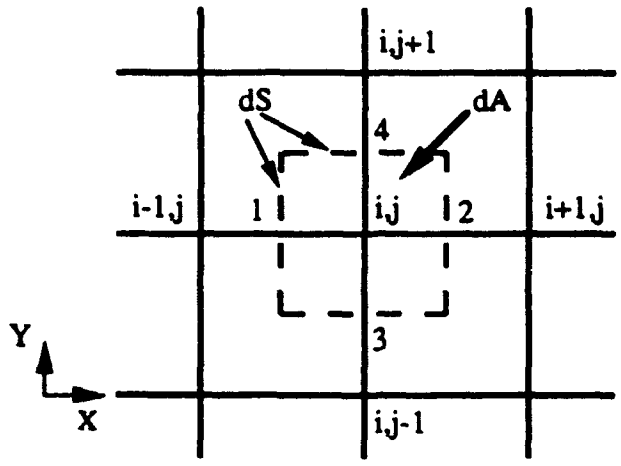

(a) Control volume element for Reynolds equation.

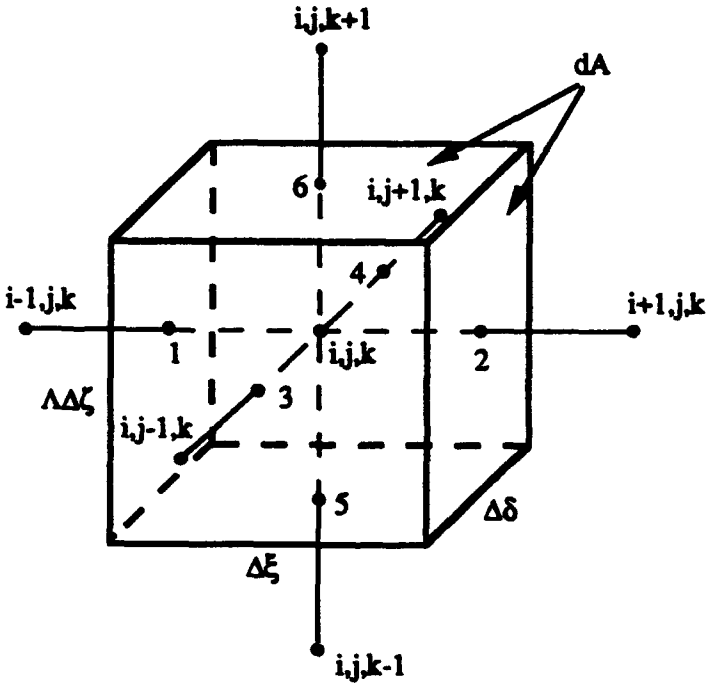

(b) Control volume element $d\bar{V}$ for the energy equation.

Figure 3. Control volume element

$$\vec{n} = -\vec{e}_Y, \quad \vec{U}\cdot\vec{n} = -V$$

$$\vec{n}\cdot\nabla T = -\frac{\partial T}{\partial \delta} + \frac{\bar{\gamma}}{\Lambda H}\frac{\partial T}{\partial \zeta} \tag{32}$$

and $dA = \Lambda H\, d\xi\, d\zeta$.

For surface 5,

$$\vec{n} = -\frac{1}{\bar{\alpha}}(\bar{\beta}\vec{e}_x + \bar{\gamma}\vec{e}_Y - \vec{e}_Z), \quad \vec{U}\cdot\vec{n} = -\frac{1}{\bar{\alpha}}(W - U\bar{\beta} - V\bar{\gamma})$$

$$\vec{n}\cdot\nabla T = \frac{1}{\bar{\alpha}}\left(\bar{\beta}\left(\frac{\partial T}{\partial \xi} - \frac{\bar{\beta}}{\Lambda H}\frac{\partial T}{\partial \zeta}\right) + \bar{\gamma}\left(\frac{\partial T}{\partial \delta} - \frac{\bar{\gamma}}{\Lambda H}\frac{\partial T}{\partial \zeta}\right) - \frac{1}{\Lambda H}\frac{\partial \Gamma}{\partial \zeta}\right) \tag{33}$$

and $dA = \sqrt{1+\bar{\beta}^2}\ \sqrt{1+\bar{\gamma}^2}\ d\xi\, d\delta$.

For surfaces 2, 4 and 6, the expressions for $\vec{n}$, $\vec{u}\cdot\vec{n}$ and $\vec{n}\cdot\nabla T$ are the same as those at surfaces 1, 3, and 5 respectively except the signs are reversed.

The volume of a control volume element is:

$$d\bar{V} = \Lambda H\, d\xi\, d\delta\, d\zeta \tag{34}$$

The resulting energy equation of a control volume in discretized form is given by:

$$-\left(\rho UT - K\frac{\Delta T}{\Delta \xi}\right)\Lambda H\ \Big|_{\,1}\ \Delta\delta\Delta\zeta + \left(\rho UT - K\frac{\Delta T}{\Delta \xi}\right)\Lambda H\ \Big|_{\,2}\ \Delta\delta\Delta\zeta$$

$$-\left(\rho VT - K\frac{\Delta T}{\Delta \delta}\right)\Lambda H\ \Big|_{\,3}\ \Delta\xi\Delta\zeta + \left(\rho VT - K\frac{\Delta T}{\Delta \delta}\right)\Lambda H\ \Big|_{\,4}\ \Delta\xi\Delta\zeta$$

$$-\frac{1}{\bar{\alpha}}\left\{(W - U\bar{\beta} - V\bar{\gamma})\rho T - K\frac{\bar{\alpha}^2}{\Lambda H}\frac{\Delta T}{\Delta \zeta}\right\}\sqrt{1+\bar{\beta}^2}\ \sqrt{1+\bar{\gamma}^2}\ \Big|_{\,5}\ \Delta\xi\Delta\delta$$

$$+\frac{1}{\bar{\alpha}}\left\{(W - U\bar{\beta} - V\bar{\gamma})\rho T - K\frac{\bar{\alpha}^2}{\Lambda H}\frac{\Delta T}{\Delta \zeta}\right\}\sqrt{1+\bar{\beta}^2}\ \sqrt{1+\bar{\gamma}^2}\ \Big|_{\,6}\ \Delta\xi\Delta\delta \;=\; S \tag{35}$$

where

$$S = K\bar{\beta}\frac{\Delta T}{\Delta\zeta}\Big|_1 \Delta\delta\Delta\zeta - K\bar{\beta}\frac{\Delta T}{\Delta\zeta}\Big|_2 \Delta\delta\Delta\zeta + K\bar{\gamma}\frac{\Delta T}{\Delta\zeta}\Big|_3 \Delta\xi\,\Delta\zeta - K\bar{\gamma}\frac{\Delta T}{\Delta\zeta}\Big|_4 \Delta\xi\Delta\zeta$$

$$+\frac{K}{\bar{\alpha}}\left[\bar{\beta}\frac{\Delta T}{\Delta\xi}+\bar{\gamma}\frac{\Delta T}{\Delta\delta}\right]\sqrt{1+\bar{\beta}^2}\ \sqrt{1+\bar{\gamma}^2}\Big|_5 \Delta\xi\Delta\delta - \frac{K}{\bar{\alpha}}\left[\bar{\beta}\frac{\Delta T}{\Delta\xi}+\bar{\gamma}\frac{\Delta T}{\Delta\delta}\right]\sqrt{1+\bar{\beta}^2}\ \sqrt{1+\bar{\gamma}^2}\Big|_6 \Delta\xi\,\Delta\delta$$

$$+S' \qquad (36)$$

The left-hand side of the equation (35) represent the convective and diffusive heat transfer. They are approximated by the power-law scheme developed by Patankar (1980). The discretized form of equation equation (35) is:

$$a_P T_P - a_E T_E - a_W T_W - a_N T_N - a_S T_S - a_T T_T - a_B T_B - S = 0 \qquad (37)$$

where, $a_E = D_2\left[0, (1-0.1\left|\frac{F_2}{D_2}\right|)^5\right] + \left[-F_2, 0\right]$

$$a_W = D_1\left[0, (1-0.1\left|\frac{F_1}{D_1}\right|)^5\right] + \left[F_1, 0\right]$$

$$a_N = D_4\left[0, (1-0.1\left|\frac{F_4}{D_4}\right|)^5\right] + \left[-F_4, 0\right]$$

$$a_S = D_3\left[0, (1-0.1\left|\frac{F_3}{D_3}\right|)^5\right] + \left[F_3, 0\right]$$

$$a_T = D_6\left[0, (1-0.1\left|\frac{F_6}{D_6}\right|)^5\right] + \left[-F_6, 0\right]$$

$$a_B = D_5\left[0, (1-0.1\left|\frac{F_5}{D_5}\right|)^5\right] + \left[F_5, 0\right]$$

and $a_P = a_E + a_W + a_N + a_S + a_T + a_B$.

The bracket [,] indicates that the larger one of the arguments is selected.

The expressions for D's are

$$D_1 = \frac{K\Lambda H}{\Delta \xi} \Big|_1 \Delta\delta\Delta\zeta$$

$$D_3 = \frac{K\Lambda H}{\Delta\delta} \Big|_3 \Delta\xi\Delta\zeta \tag{38}$$

$$D_5 = K \frac{\bar{\alpha}}{\Lambda H} \frac{\sqrt{1+\bar{\beta}^2}\ \sqrt{1+\bar{\gamma}^2}}{\Delta\zeta} \Big|_5 \Delta\xi\Delta\delta$$

The expression for the F's are:

$$F_1 = \rho U \Lambda H \Big|_1 \Delta\delta\Delta\zeta,$$

$$F_3 = \rho V \Lambda H \Big|_3 \Delta\xi\Delta\zeta, \tag{39}$$

$$F_5 = \frac{\rho}{\bar{\alpha}} \left(W - U\bar{\beta} - V\bar{\gamma}\right) \sqrt{1+\bar{\beta}^2}\sqrt{1+\bar{\gamma}^2} \Big|_5 \Delta\xi\Delta\delta.$$

The expressions for the D's and F's on the surfaces 2,4, and 6 are identical to those on the surfaces 1,3 and 5 respectively.

4. Numerical Procedure

Generally, to obtain a numerical solution to the problem of compressible thermal EHD lubrication of rolling/sliding contact, the discretized Reynolds and the elasticity equations were solved using an iterative technique. The iterative technique required an underrelaxation factor to obtain an accurate and converged solution. However, for the heavily loaded conditions, this underrelaxation factor was usually very small, which caused the rate of convergence of the numerical scheme to be extremely low.

In order to reduce the computing time and increase the accuracy, the multilevel multigrid technique was employed in this analysis. The multigrid procedure used is similar to that implemented by Lubrecht (1987) for the isothermal EHD lubrication of point contacts. In order for the multigrid method to be successful it is essential to use a relaxation scheme which has a good error smoothing property. In this investigation, since the Reynolds equation is nonlinear, point Gauss-Seidel-Newton relaxation scheme was used. The iterative formula for the pressure is:

$$(P_{i,j})^{new} = (P_{i,j})^{old} - \frac{\omega f_{i,j}}{\frac{\partial f_{i,j}}{\partial P_{i,j}} + \frac{\partial f_{i,j}}{\partial \eta_{i+\frac{1}{2},j}} \frac{\partial \eta_{i+\frac{1}{2},j}}{\partial P_{i,j}} + \frac{\partial f_{i,j}}{\partial \eta_{i-\frac{1}{2},j}} \frac{\partial \eta_{i-\frac{1}{2},j}}{\partial P_{i,j}} + \frac{\partial f_{i,j}}{\partial \eta_{i,j+\frac{1}{2}}} \frac{\partial \eta_{i,j+\frac{1}{2}}}{\partial P_{i,j}} + \frac{\partial f_{i,j}}{\partial \eta_{i,j-\frac{1}{2}}} \frac{\partial \eta_{i,j-\frac{1}{2}}}{\partial P_{i,j}} + \frac{\partial f_{i,j}}{\partial H_{i,j}} \frac{\partial H_{i,j}}{\partial P_{i,j}} + \frac{\partial f_{i,j}}{\partial H_{i-1,j}} \frac{\partial H_{i-1,j}}{\partial P_{i,j}}} \quad (40)$$

where, $f_{i,j}$ is the residual of the Reynolds equation at node (i,j) and ω is the underrelaxation factor. The subscript $(i+\frac{1}{2})$ denotes the functional value at the midpoint between i and i+1. Similarly, $(j+\frac{1}{2})$ also denotes the functional value at the mid point between j and j+1.

The energy equation is also relaxed with the point Gauss-Seidel-Newton relaxation scheme. The viscosity in the shear heating term is an exponential function of the temperature, therefore, the change in energy equation with respect to viscosity is included in the relaxation

scheme. The iterative formula for the temperature is:

$$(T_{i,j,k})^{new} = (T_{i,j,k})^{old} - \frac{\omega\, g_{i,j,k}}{\frac{\partial g_{i,j,k}}{\partial T_{i,j,k}} + \frac{\partial g_{i,j,k}}{\partial \eta_{i,j,k}} \frac{\partial \eta_{i,j,k}}{\partial T_{i,j,k}}} \tag{41}$$

where $g_{i,j,k}$ is the residual of the energy equation and ω is the underrelaxation factor. The complete description of the multilevel multigrid technique can be found in numerous literature (e.g. Brandt, 1984). Therefore, the explanation of the multigrid procedure is not presented here.

Figure 4 illustrates the flowchart for the computational procedure that was used for calculating the pressure, film thickness and the temperature distribution within the lubricant film. First, the Hertzian pressure distribution is used as an initial guess for the Reynolds equation. With the viscosity, density and film thickness calculated, the discretized Reynolds equation is relaxed. The H_o value is modified at each relaxation to reduce the residual of the force balance equation. After the Reynolds equation relaxation is finished, the discretized energy equation is relaxed. The ambient temperature is used as the initial guess for the temperature. The pressure, film thickness are fixed during the relaxation of the energy equation. Then the pressure, film thickness and temperature are transferred to the next level according to the prefixed multigrid cycle path. The 2V cycle and Full Approximate Scheme was incorporated in the multigrid path. The residuals of the Reynolds equation, the film thickness equation, the force balance equation and the energy equation are also transferred. The film thickness is much smaller than the other dimensions, therefore, semicoarsening was used to transfer the residuals and the field variables.

5. Interactive Computer Graphics

An interactive computer graphics package was developed for use in the design and analysis of EHD lubrication of rolling/sliding circular and elliptic contacts. The graphics package provides a user friendly interactive computer graphics interface with the multigrid

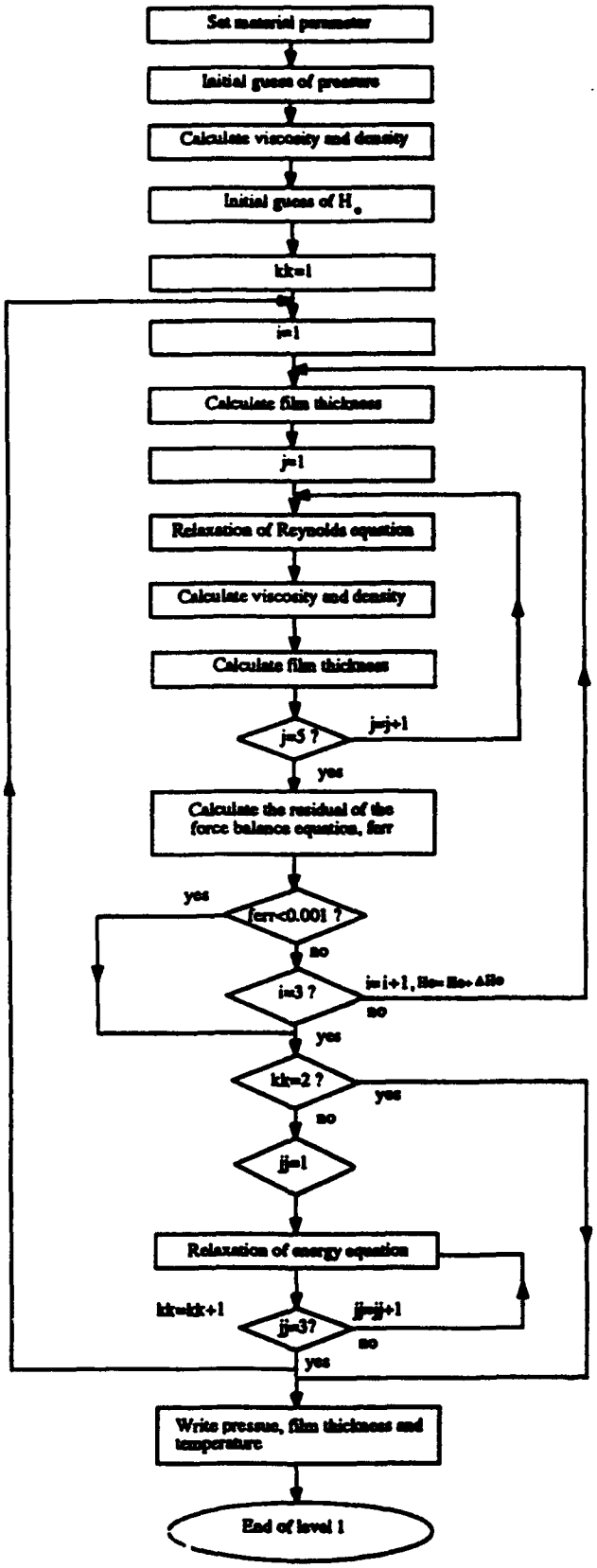

Figure 4. Flow chart for thermal EHD solution at level one.

multilevel EHD numerical model. The graphics package allows the user to input the boundary conditions and performance parameters (i.e., load, speed, material parameter, etc.) using graphics pictorial representation of the problem. Once an EHD model has been analyzed, the graphics package enables the user to critically examine the results. It provides an environment where the user can view several results (pressure, temperature, etc.) at once. This allows the critical examination of the effects of various performance parameters on the output results.

Figure 5 illustrates two spheres in contact, the input for the two spheres and the properties of the lubricant separating the surfaces. The properties of the solids or the lubricant can simply be changed by placing the arrow with the mouse cursor on the appropriate sphere, lubricant, etc. and pressing the mouse button. Figures 6 and 7 depict other geometries which the EHD lubrication model can analyze. Figure 6 illustrates two ellipsoid in contact where the radius of curvature in the rolling direction (x) is smaller than in the y-direction. However, Figure 7 demonstrates the condition where the radius of curvature in the rolling direction is larger than in the y-direction. Note that the ellipticity ratio for the conditions considered in Figures 6 and 7 are 1.581 and 0.6325, respectively. Figure 8 depicts the solid properties for two spheres in contact. In order to change any of the material properties, the cursor is placed in the appropriate box and the mouse button pressed. A prompt appears and the change can be entered. Every time any of the properties of the solid, lubricant, etc., are changed, the program updates the geometry and the nondimensional parameters to be used in the EHD numerical model. When all of the changes have been entered to the default data base, the EHD model can be used to analyze the input data by placing the cursor in the "process" menu bar and clicking on "Run EHD Program." A box will appear where the output of the analysis can be stored. Once the output file has been entered, the computer aided design/graphics program prompts the EHD numerical model to run the

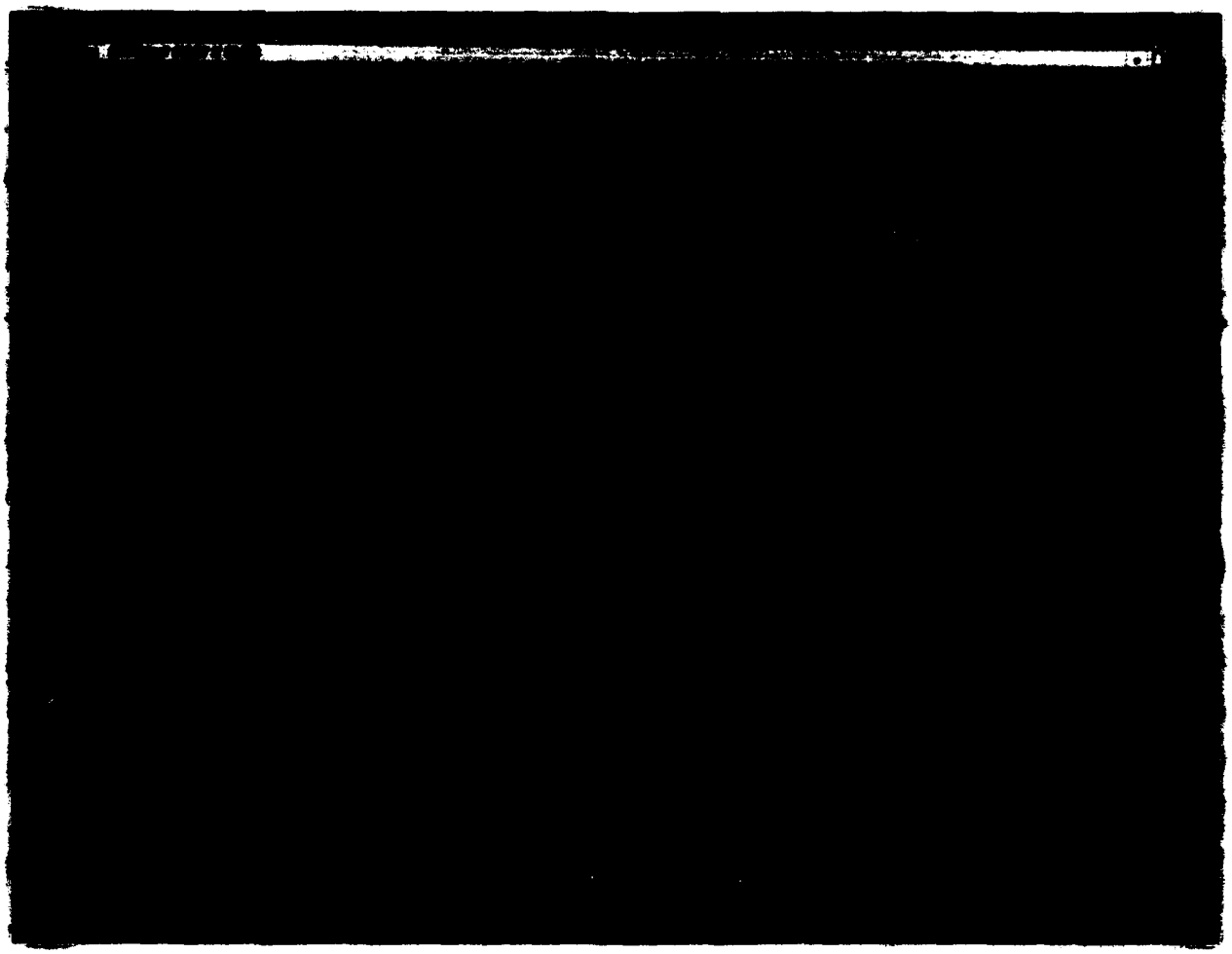

Figure 5. Geometry, Material and Lubricant Selection for EHD Analysis, Two Spherical Bodies in Contact.

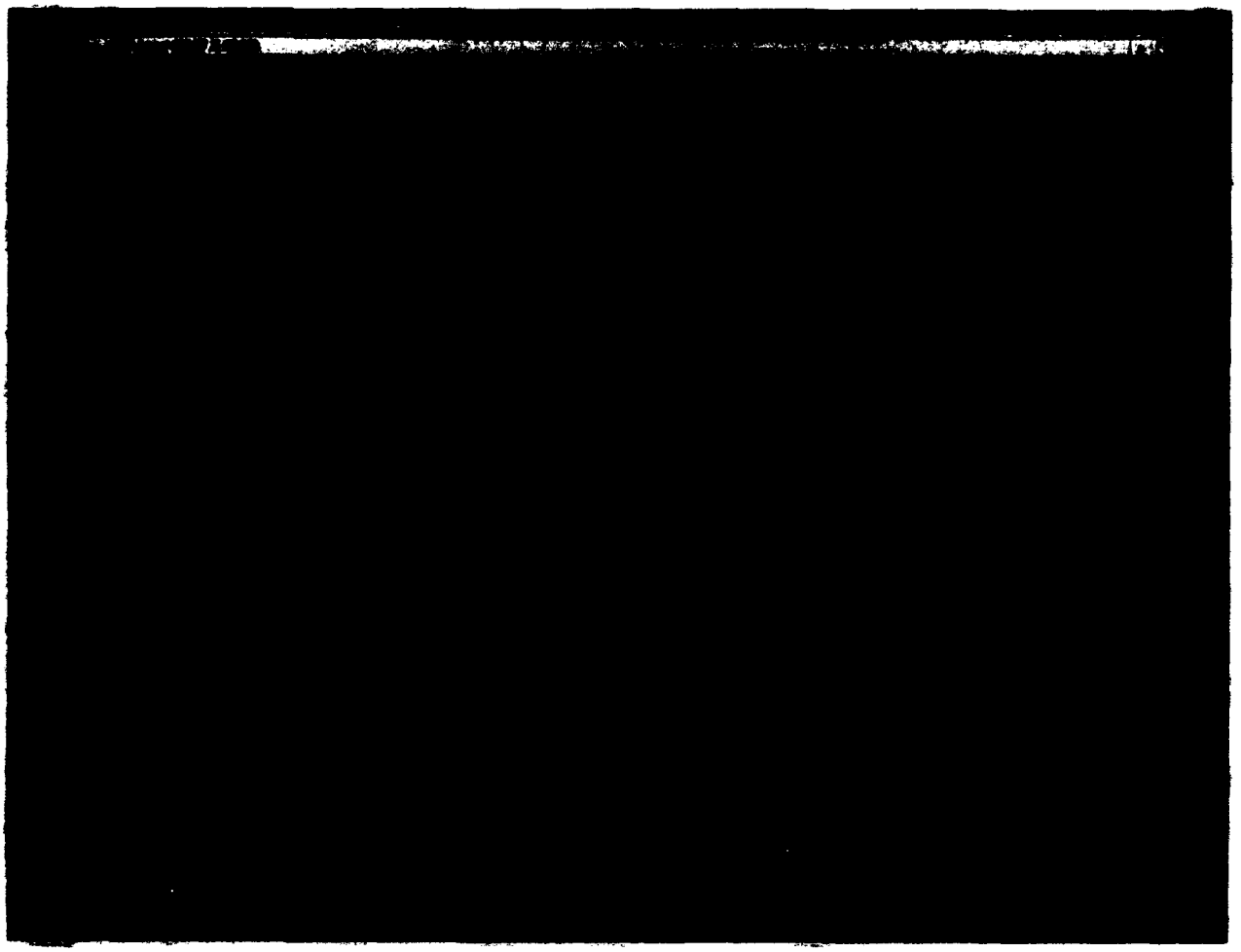

Figure 6. Geometry, Material and Lubricant Selection for EHD Analysis, Two Ellipsoidal Bodies in Contact. (Ellipticity ratio = 1.581)

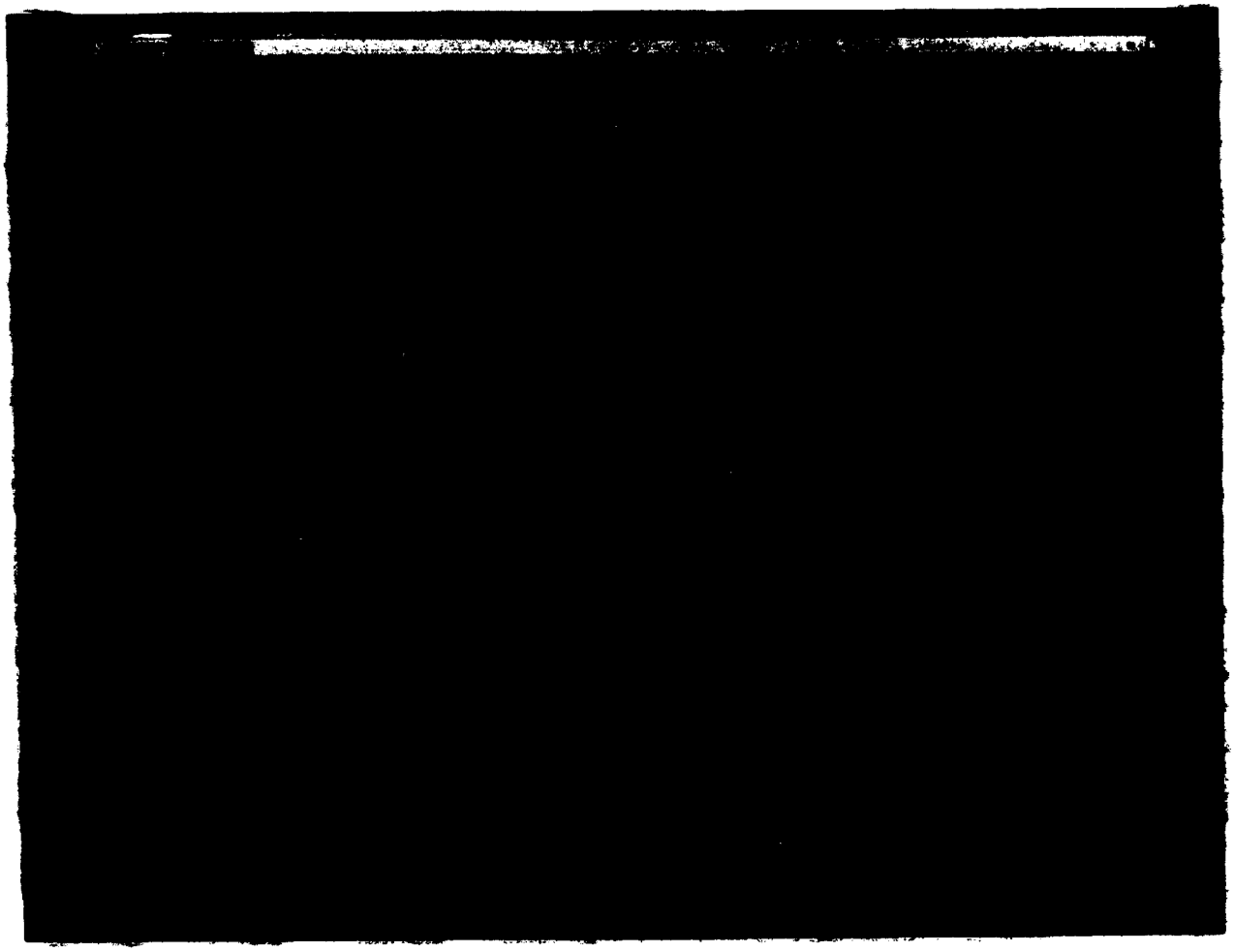

Figure 7. Geometry, Material and Lubricant Selection for EHD Analysis, Two Ellipsoidal Bodies in Contact. (Ellipticity ratio = 0.6325)

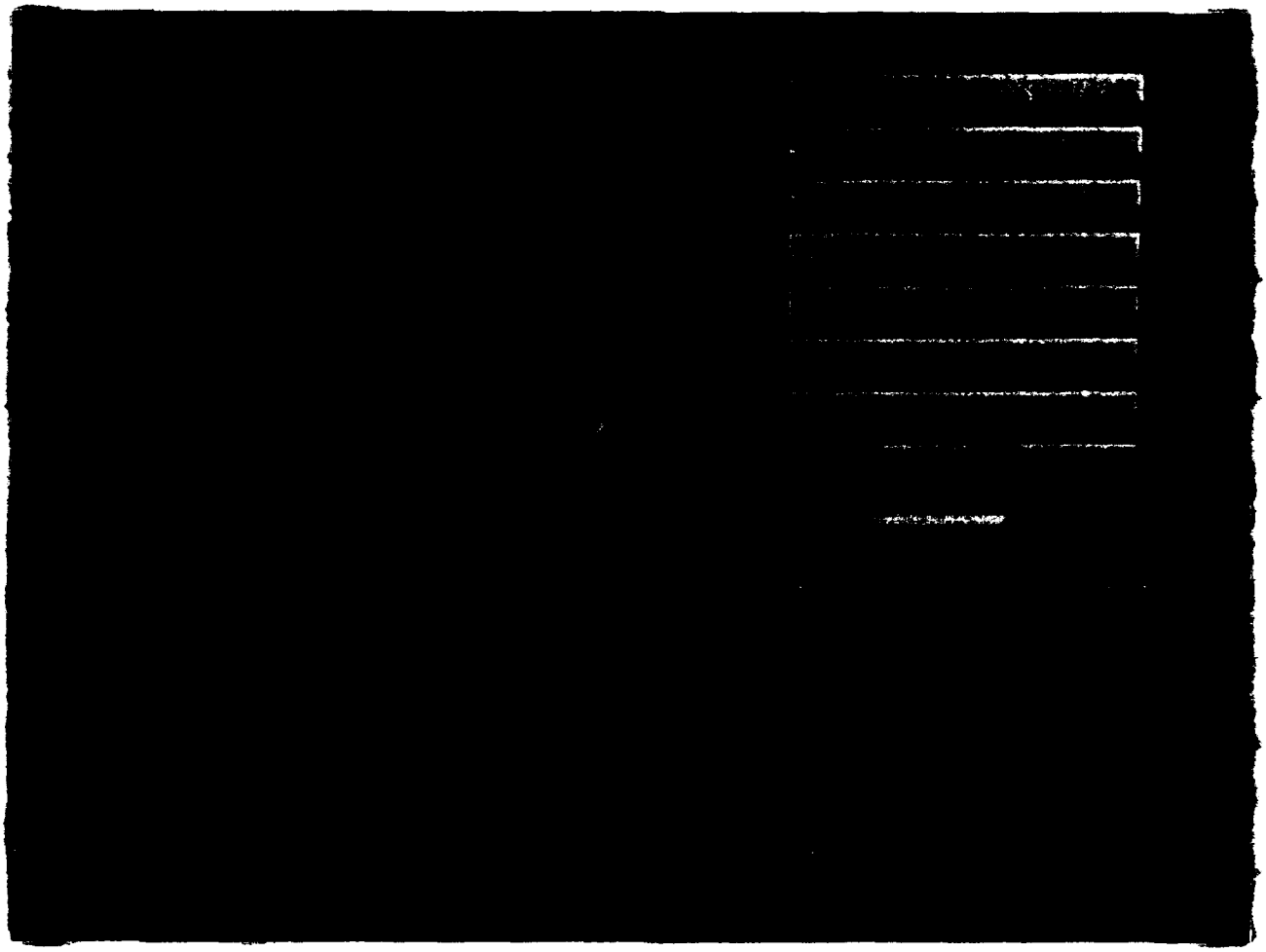

Figure 8. Material Selection and the List of Variables That can be Changed.

particular data get developed.

Figures 9 through 15 depict the results for the conditions shown in Figures 5 through 7. Figures 9 through 11 illustrate the pressure, temperature, film thickness contour and the volumetric rendering of the shear stress in the xz direction. Figure 9 allows the user to quickly examine the location and relative magnitude of maximum pressure and temperature. The user can manipulate and rotate these figures and view them from any direction. He/she can view contour and surface plots of all of the output variable (i.e., velocity, shear stress, etc.). The results can be viewed in Metric or nondimensional. Figure 10 illustrates the contour plot of the film thickness. However, the user can view the contour plot of any of the output results (i.e., temperature, pressures, shear stress, etc.) by placing the mouse button on the "parameter" in the menu bar and choose the appropriate variable. The user can also choose the number of color contours (5 to 200) in the menu bar. Figure 11 is the volumetric rendering of the shear stress results. In this case the iso-surface results for a range chosen by the user in the lubricant film is presented. This will allow the user to quickly determine the magnitude and location of the parameter of interest in the volumetric region that the lubricant film occupies.

Figures 12 and 13 illustrate the pressure, temperature and film contour for the condition described in Figure 6. In this case the ellipticity ratio is 1.581. The pressure exhibits a pressure spike region around the edge and the back of the contact near the exit region. The temperature contour (Figure 12) shows that the temperature reaches its maximum in the center of the contact. Figure 13 depicts the contour plot of the film thickness. Note the general horseshoe shape.

Figures 14 and 15 depict the results for the conditions considered in Figure 7. In this the ellipticity ratio is 0.6325 which indicates the width of the contact in the rolling direction (x) is larger than the width of the contact in the y-direction. In this case, again the pressure exhibits

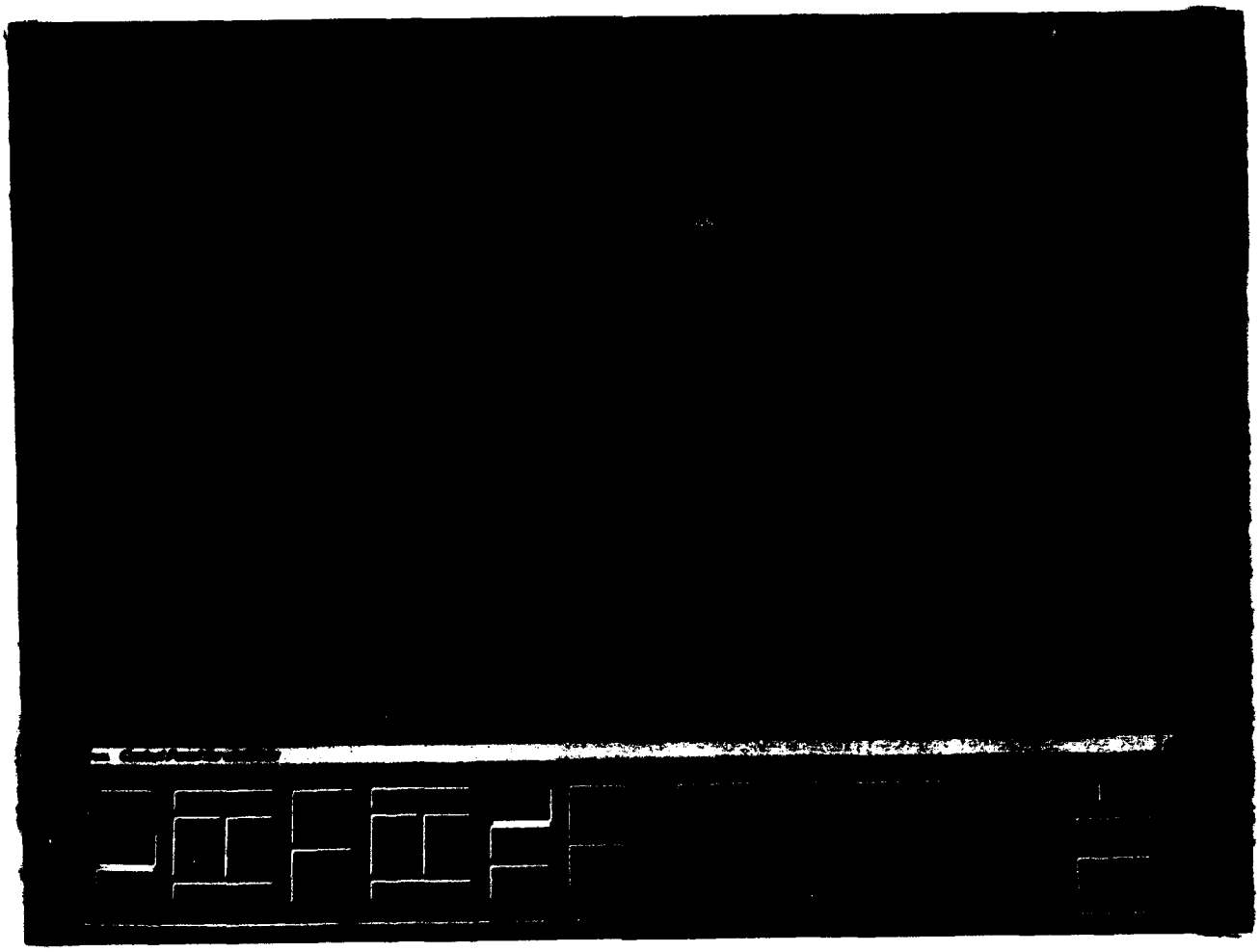

Figure 9. Pressure and Color Contour of Temperature in an EHD Lubrication of Circular Contact.

Figure 10. Color Contour of the Film Thickness in an EHD Lubrication of Circular Contact.

Figure 11. Three Dimensional Volume Rendering of Shear Stress Iso-Surfaces.

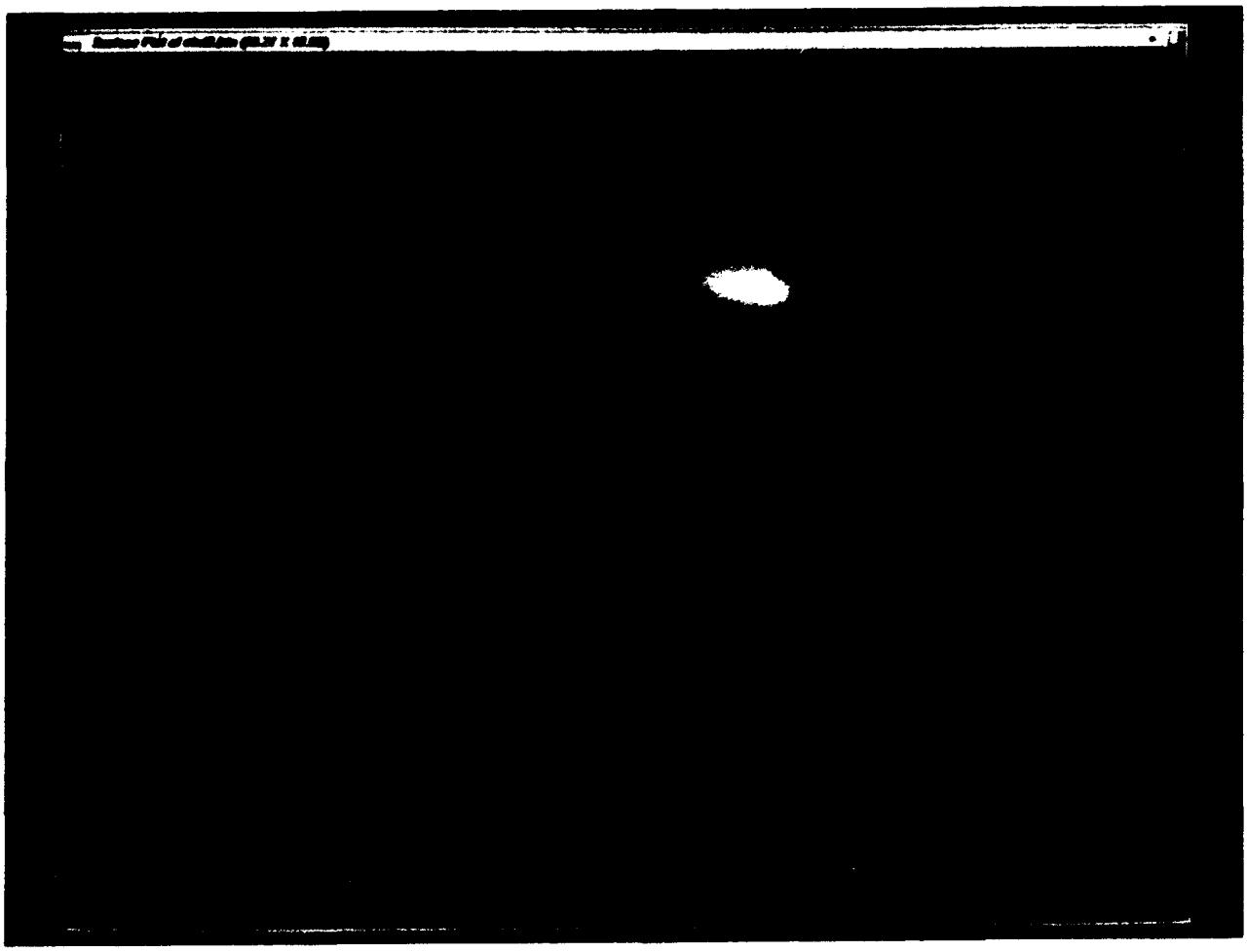

Figure 12. Pressure and Color Contour of Temperature in an EHD Lubrication of Elliptic Contact. (Ellipticity Ratio - 1.581)

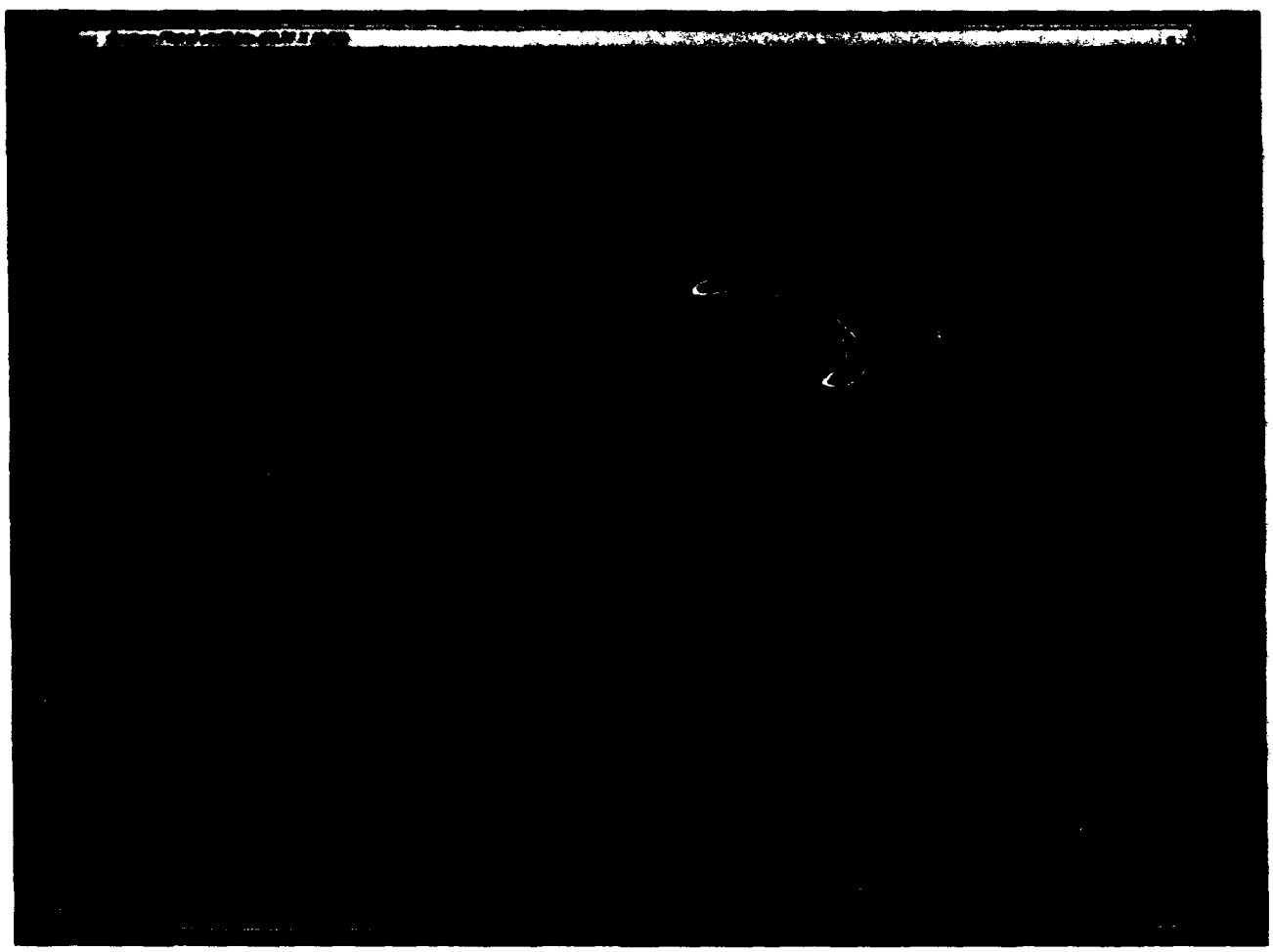

Figure 13. Color Contour of the Film Thickness in an EHD Lubrication of Elliptic Contact. (Ellipticity Ratio - 1.581)

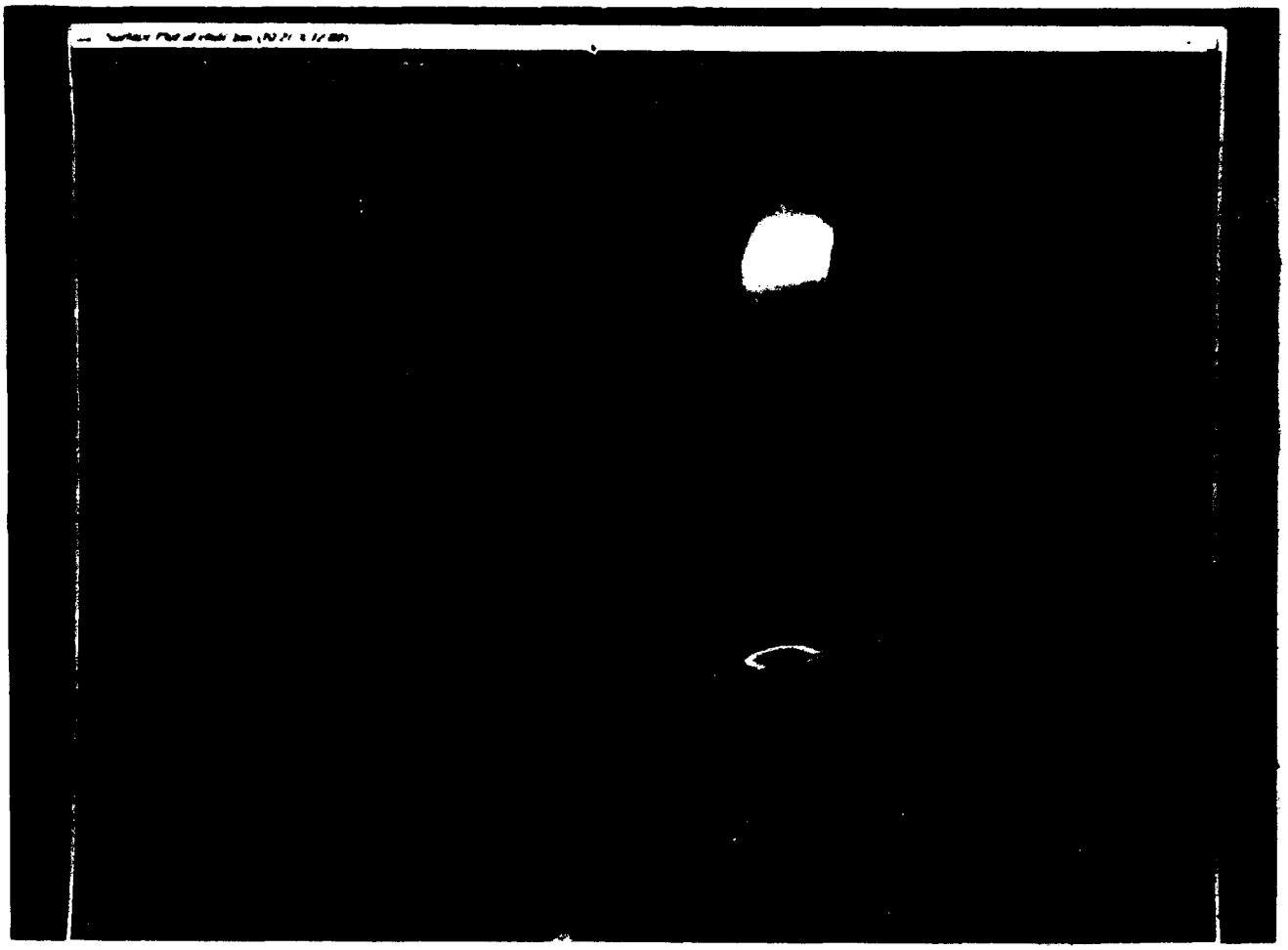

Figure 14. Pressure and Color Contour of Temperature in an EHD Lubrication of Elliptic Contact. (Ellipticity Ratio - 0.6325)

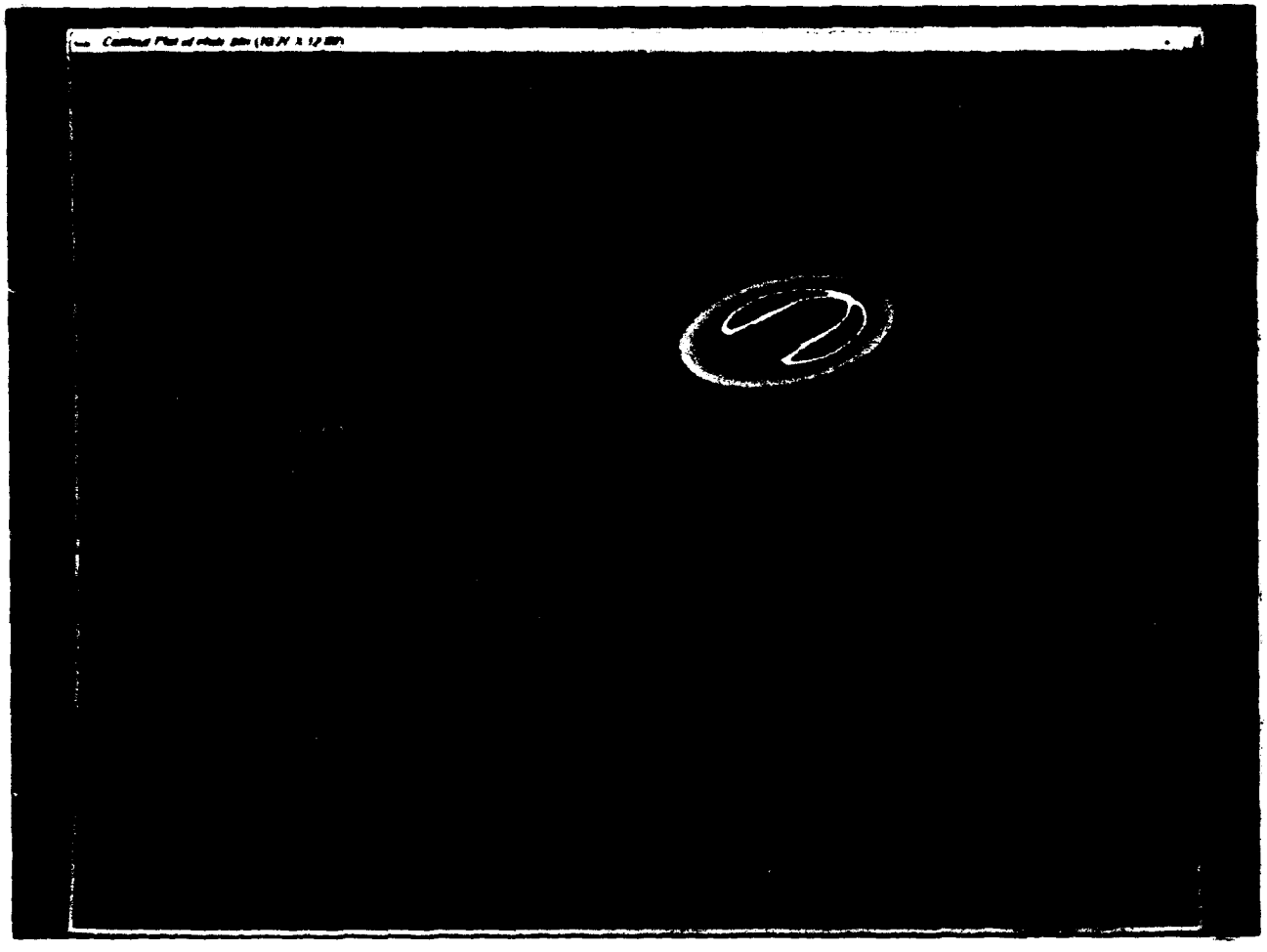

Figure 15. Color Contour of the Film Thickness in an EHD Lubrication of Elliptic Contact. (Ellipticity Ratio - 0.6325)

the region of pressure spike and the temperature is maximum at the center of the contact.

6. Conclusion

A robust and fast converging numerical technique to solve the simultaneous system of two-dimensional Reynolds, elasticity and three-dimensional energy equations has been developed. The numerical technique, the coordinate transformation, as well as the iterative scheme, have been presented. An interactive computer graphics model was developed to provide a user friendly environment for the design and analysis of EHD lubrication of rolling/sliding circular and elliptic contacts. The package is fast converging, flexible and provides a user friendly design package to investigate heavily loaded lubricated contacts.

REFERENCES

Blahey, A. G., and Schneider, G. E., 1986, "A Numerical Solution of the Elastohydrodynamic Lubrication of Elliptical Contacts with Thermal Effects," Proceedings of 13th Leeds-Lyon Symposium on Tribology, Held in The University of Leeds, England, 8-12 September 1986

Brandt, A., 1984, Multigrid Technique: 1984 Guide with Applications to Fluid Dynamics, GMD-Studien Nr. 85, Gesellschaft für Mathematik und Datenverarbeitung MBH, Bonn, Germany, May 1984

Brüggemann, H. and Kollmann, F. G., 1982, " A Numerical Solution of the Thermal Elastohydrodynamic Lubrication in an Elliptic Contact," Journal of Lubrication Technology, Vol. 104, No. 3, pp. 392-400

Carslaw, J.W., and Jaeger, J.C., 1959, Conduction of Heat in Solids, Oxford University Press, London

Cheng, H. S., 1965, "A Refined Solution to the Thermal Elastohydrodynamic Lubrication of Rolling Sliding Contact," Trans. ASLE, Vol. 8, No. 4, pp. 397-410

Dowson, D., and Higginson, G. R., 1966, Elastohydrodynamic Lubrication, Pergamon Press

Dowson, D., 1962, "A Generalized Reynolds Equation for Fluid Film Lubrication," International Journal of Mechanical Science, Vol. 4, pp 159-164

Evans, H.P., and Snidle, R.W., 1982, " The Elastohydrodynamic Lubrication of Point Contacts at Heavy Loads," Proceedings of Royal Society of London, Series A, Vol. 382, PP 183-199

Faghri, M., Sparrow, E. M. and Prata, A. T., 1984, "Finite-Difference Solutions of Convection-Diffusion Problems in Irregular Domains, Using A Nonorthogonal Transformations," Numerical Heat Transfer, Vol 17, pp. 183-209

Hamrock, B.J., and Dowson, D.,1977, " Isothermal Elastohydrodynamic Lubrication of Point Contacts, Part III-Fully Flooded Results," ASME Journal of Lubrication Technology, Vol. 99, No. 2, pp 204-216,

Houpert, L., 1985, "New Results of Traction Force Calculations in EHD Contacts," Trans. ASME, Journal of Lubrication Technology, Vol. 107, pp 241-248

Lubrecht, A. A., Napel, W. E., and Bosman, R., 1987, " Multigrid, An Alternative method of Solution for the Two-Dimensional Elastohydrodynamically Lubricated Point Contact Calculations," Journal of Tribology, Vol. 112, No. 4, pp. 1507-1518

Murch, L. E., and Wilson, W. R. D., 1975, "A Thermal Elastohydrodynamic Inlet Zone Analysis," Trans. ASME, Vol. 97, No. 2, pp. 212-216

Patankar, S. V., 1980, Numerical Heat Transfer and Fluid Flow, Hemisphere Publishing Co.,

Washington

Ranger, A.P., Ettles, C.M.M., and Cameron, A., 1975, "The Solution of Point Contact Elastohydrodynamic Problem," Proceedings of Royal Society of London, Series A, Vol. 346, pp. 227-244

Roelands, C. J. A., Vlugter, J. C., and Watermann, H. I., 1963, "The Viscosity Temperature Pressure Relationship of Lubricating Oils and Its Correlation with Chemical Constitution," ASME Journal of Basic Engineering, p. 601

Sadeghi, ıd Dow, T. A., 1987, "Thermal Effects in Rolling/Sliding Contacts: Part 2 - Analysis ot Thermal Effects in Fluid Film," Journal of Tribology, Vol. 109, No. 3, p. 109

Sadeghi, F. and Sui, P., 1990, "Thermal Elastohydrodynamic Lubrication of Rolling/Sliding Contacts," Journal of Tribology, Vol. 112, No. 2, pp. 189-195

Sherman, F., 1990, Viscous Flow, McGraw-Hill, New York

Sternlicht, B., Lewis, P., and Flynn, P., 1961, "Theory of Lubrication and failure of Rolling Contacts," ASME Journal of Basic Engineering, pp. 213-226

Zhu, D. and Cheng, H.S., 1989, " An Analysis and Computational Procedure for EHL Film Thickness, Friction and Flash Temperature in Line and Point Contacts," Tribology Transactions, Vol 32, pp 364-370

Zhu, Dong and Wen, Shi-Zhu, 1984, " A Full Numerical Solution for the Thermoelastohydrodynamic Problem of Elliptical Contacts," Journal of Lubrication Technology, Vol. 106, pp. 246-254